DISCRETIZATION OF THE '59 FENDER BASSMAN TONE STACK

David T. Yeh, Julius O. Smith

Center for Computer Research in Music and Acoustics (CCRMA)
Stanford University, Stanford, CA
{dtyeh|jos}@ccrma.stanford.edu

ABSTRACT

The market for digital modeling guitar amplifiers requires that the digital models behave like the physical prototypes. A component of the iconic Fender Bassman guitar amplifier, the tone stack circuit, filters the sound of the electric guitar in a unique and complex way. The controls are not orthogonal, resulting in complicated filter coefficient trajectories as the controls are varied. Because of its electrical simplicity, the tone stack is analyzed symbolically in this work, and digital filter coefficients are derived in closed form. Adhering to the technique of virtual analog, this procedure results in a filter that responds to user controls in exactly the same way as the analog prototype. The general expressions for the continuous-time and discrete-time filter coefficients are given, and the frequency responses are compared for the component values of the Fender '59 Bassman. These expressions are useful implementation and verification of implementations such as the wave digital filter.

1. INTRODUCTION

1.1. Motivation

The guitar amplifier is an essential component of the electric guitar sound, and often musicians collect several amplifiers for their tonal qualities despite the space they occupy. As digital signal processors (DSP) continue to improve in performance, there is great interest in replacing expensive and bulky vacuum tube guitar amplifiers with more flexible and portable digital models. A digital model of a guitar amplifier allows a variety of sounds associated with different amplifiers to be selected from a single amplifier unit. One company, Line 6 bases its main product line upon this concept, and other companies such as Roland (Boss), Korg (Vox), Harman International (Digitech) have competing products.

Most commercially viable digital guitar processing products use simplified models of the distortion and filters to reduce DSP power consumption and reduce manufacturing costs. The distortion is typically a nonlinear transfer curve, accompanied by digital filtering that is manually tuned to match the sound of a famous guitar amplifier.

With no pressure to produce a commercially successful product, this research takes a different approach. The goal of this research is to see how accurate a sound can be achieved through careful physical modeling of the vacuum tube amplifier and to provide a physical basis for the digital model and parameters. Because the tone stack is a passive, linear component, it is a straightforward starting point.

1.2. Properties of the tone stack

Commonly found in many guitar amplifiers, especially those that derive from the Fender design, the tone stack filters the signal of the guitar in a unique and non-ideal way. The user can adjust Treble, Middle, and Bass controls to modify the gain of the respective frequency bands. However, these controls are not orthogonal, and changing some controls affects the other bands in a complex way.

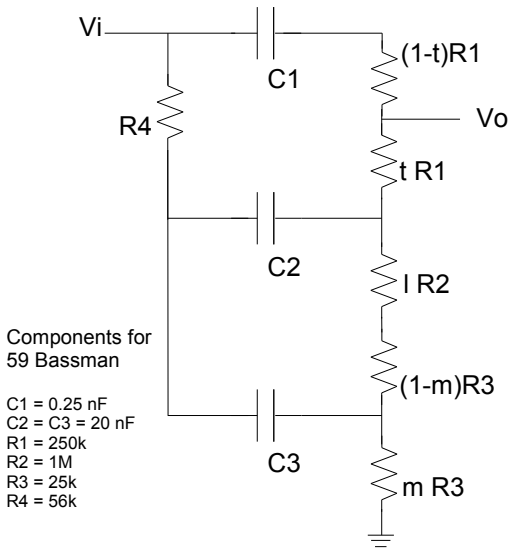

Figure 1: *Tone stack circuit with component values.*

The full Bassman schematic can be easily found online [1] and in guitar amplifier books. While other guitar amplifiers may vary slightly, in the Bassman type designs, the tone stack is found after the preamplifier stages and before the phase splitter. In good designs, the tone stack is preceded by a cathode follower to buffer the input and reduce variations in frequency response due to loading. Typically this presents a $1k\Omega$ load to the input and the phase splitter stage presents a $1M\Omega$ load to the output.

The Fender '59 Bassman tone stack circuit is shown in Fig. 1. The Treble, Middle, and Bass knobs are potentiometers, which have been modeled here as parameterized resistors. The Treble and Middle controls use linear potentiometers, while the Bass control uses a logarithmic taper potentiometer. In this paper, t and m correspond to the Treble and Middle controls and range in value from $[0, 1]$. The Bass control, l, also ranges from $[0, 1]$, but is swept logarithmically.

1.3. Related work

Fender Musical Instruments has a patent to simulate various tone stacks using an active analog filter and an interpolation scheme to extract the filter coefficients [2]. Line 6 also models the behavior of the Bassman tone stack as indicated in the BassPODxt manual. However, their implementation is proprietary knowledge. An open source guitar effects plug-in suite for Linux, CAPS [3], uses shelving filters instead of the tone stack.

Previous works have analyzed the tone stack using numerical circuit analysis techniques. This involves setting up the nodal equations as a matrix and inverting it or performing Gaussian elimination to find the solution. For example, the Tone Stack Calculator from Duncan Amps will plot the frequency response of various tone stacks given the control settings [4]. Kuehnel in his book analyzed the mesh equations of the tone stack, using low frequency and high frequency circuit approximations [5]. He also compares these simplified equations to the numerical solutions solved by inverting the matrix of the mesh equations. While the approximations make the circuit analysis more tractable, they do not reduce the order of the equations and do not make the discretization of the filter any easier.

Because the tone stack is a third-order passive network of resistors and capacitors (RC), its filter coefficients can be derived and modeled exactly in the digital domain as shown later. The approach taken here is to find the continuous time transfer function of the circuit analytically and to discretize this by the bilinear transformation. This provides a means of updating the digital filter coefficients based upon changes to the tone controls.

The passive filter circuit also is suited to implementation as a wave digital filter (WDF)[6]. This approach can easily model standard components such as inductors, capacitors, and resistors. The analytical form derived here can be used for comparison with and verification of the WDF implementation.

2. DISCRETIZATION PROCEDURE

2.1. Symbolic Circuit Analysis

Because this is a relatively simple circuit, it is amenable to exact symbolic analysis by mathematical Computer Aided Design (CAD) software such as Mathematica (Wolfram Research, Inc., Champaign, IL). The filter coefficients can thus be found without any approximations. Performing symbolic nodal analysis on this circuit yields the following input/output transfer function $H(s) = V_o(s)/V_i(s)$, where V_o is the output and V_i is the input as in Fig. 1.

$$H(s) = \frac{b_1 s + b_2 s^2 + b_3 s^3}{a_0 + a_1 s + a_2 s^2 + a_3 s^3}, \tag{1}$$

where

$$b_1 = tC_1R_1 + mC_3R_3 + l(C_1R_2 + C_2R_2) + (C_1R_3 + C_2R_3),$$

$$\begin{aligned} b_2 = {} & t(C_1C_2R_1R_4 + C_1C_3R_1R_4) - m^2(C_1C_3R_3^2 + C_2C_3R_3^2) \\ & + m(C_1C_3R_1R_3 + C_1C_3R_3^2 + C_2C_3R_3^2) \\ & + l(C_1C_2R_1R_2 + C_1C_2R_2R_4 + C_1C_3R_2R_4) \\ & + lm(C_1C_3R_2R_3 + C_2C_3R_2R_3) \\ & + (C_1C_2R_1R_3 + C_1C_2R_3R_4 + C_1C_3R_3R_4), \end{aligned}$$

$$\begin{aligned} b_3 = {} & lm(C_1C_2C_3R_1R_2R_3 + C_1C_2C_3R_2R_3R_4) \\ & - m^2(C_1C_2C_3R_1R_3^2 + C_1C_2C_3R_3^2R_4) \\ & + m(C_1C_2C_3R_1R_3^2 + C_1C_2C_3R_3^2R_4) \\ & + tC_1C_2C_3R_1R_3R_4 - tmC_1C_2C_3R_1R_3R_4 \\ & + tlC_1C_2C_3R_1R_2R_4, \end{aligned}$$

$$a_0 = 1,$$

$$\begin{aligned} a_1 = {} & (C_1R_1 + C_1R_3 + C_2R_3 + C_2R_4 + C_3R_4) \\ & + mC_3R_3 + l(C_1R_2 + C_2R_2), \end{aligned}$$

$$\begin{aligned} a_2 = {} & m(C_1C_3R_1R_3 - C_2C_3R_3R_4 + C_1C_3R_3^2 \\ & + C_2C_3R_3^2) + lm(C_1C_3R_2R_3 + C_2C_3R_2R_3) \\ & - m^2(C_1C_3R_3^2 + C_2C_3R_3^2) + l(C_1C_2R_2R_4 \\ & + C_1C_2R_1R_2 + C_1C_3R_2R_4 + C_2C_3R_2R_4) \\ & + (C_1C_2R_1R_4 + C_1C_3R_1R_4 + C_1C_2R_3R_4 \\ & + C_1C_2R_1R_3 + C_1C_3R_3R_4 + C_2C_3R_3R_4), \end{aligned}$$

$$\begin{aligned} a_3 = {} & lm(C_1C_2C_3R_1R_2R_3 + C_1C_2C_3R_2R_3R_4) \\ & - m^2(C_1C_2C_3R_1R_3^2 + C_1C_2C_3R_3^2R_4) \\ & + m(C_1C_2C_3R_3^2R_4 + C_1C_2C_3R_1R_3^2 \\ & - C_1C_2C_3R_1R_3R_4) + lC_1C_2C_3R_1R_2R_4 \\ & + C_1C_2C_3R_1R_3R_4, \end{aligned}$$

where t is the Treble (or "top") control, l is the Bass (or "low") control, and m is the "middle" control.

2.2. Verification with SPICE circuit simulation

To verify the correctness of this expression, Figs. 2 and 3 compare the frequency response with the result from the AC analysis of SPICE[1] simulation at the settings $t = m = l = 0.5$. The plots show an exact match, verifying that Eqn. 1 is a complete and exact expression for the transfer function of the tone stack. SPICE simulation also determined that the frequency response was unaffected by the typical loading of $1k\Omega$ at the input and $1M\Omega$ at the output.

2.3. Discretization by Bilinear Transform

The continuous time transfer function was discretized by the bilinear transformation. Substituting $s = c\frac{1-z^{-1}}{1+z^{-1}}$ in (1) using Mathematica yields

$$H(z) = \frac{B_0 + B_1 z^{-1} + B_2 z^{-2} + B_3 z^{-3}}{A_0 + A_1 z^{-1} + A_2 z^{-2} + A_3 z^{-3}} \tag{2}$$

where

$$\begin{aligned} B_0 &= -b_1c - b_2c^2 - b_3c^3, \\ B_1 &= -b_1c + b_2c^2 + 3b_3c^3, \\ B_2 &= b_1c + b_2c^2 - 3b_3c^3, \\ B_3 &= b_1c - b_2c^2 + b_3c^3, \\ A_0 &= -a_0 - a_1c - a_2c^2 - a_3c^3, \\ A_1 &= -3a_0 - a_1c + a_2c^2 + 3a_3c^3, \\ A_2 &= -3a_0 + a_1c + a_2c^2 - 3a_3c^3, \\ A_3 &= -a_0 + a_1c - a_2c^2 + a_3c^3\,. \end{aligned}$$

[1] http://bwrc.eecs.berkeley.edu/Classes/IcBook/SPICE/

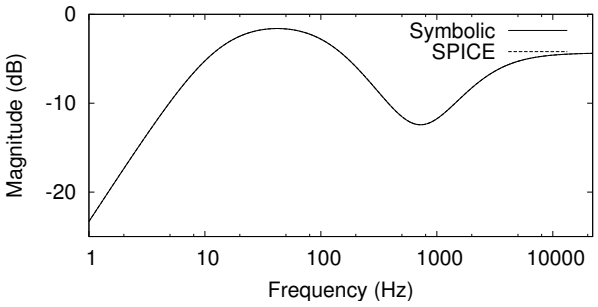

Figure 2: *Comparison of magnitude response between analytical expression and SPICE for* $t = l = m = 0.5$.

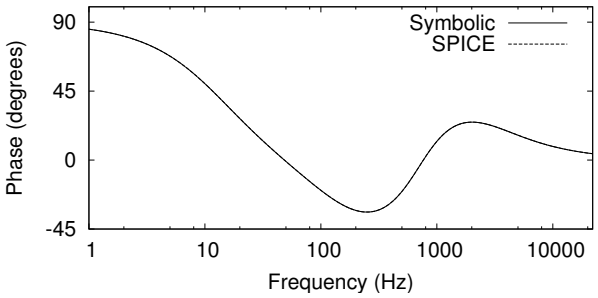

Figure 3: *Comparison of phase response between analytical expression and SPICE for* $t = l = m = 0.5$.

We used $c = 2/T$, which is ideal for frequencies close to DC.

3. ANALYSIS OF RESULTS

3.1. Comparison of continuous- and discrete- time responses

Figs. 4–6 show the discrete- and continuous-time transfer functions compared for various settings of t, m, and l. Each figure shows a different setting of l, and each sub-figure shows a different setting of m. In each plot, the treble control, t, was swept from 0.0001 to 0.5 to 0.9999 and can be distinguished by the corresponding increase in high frequency response.

The discretized filter used a sampling frequency of 44.1 kHz as typical for audio systems. The plots for $f_s = 44.1$ kHz show an excellent match through 10 kHz. The discrete and continuous plots are practically indistinguishable, with some deviations at the higher frequencies, as expected with the bilinear transform.

Because commercial guitar processing units use a lower sampling rate for cost savings, Figs. 7–9 show the same plots as above with f_s reduced to 20 kHz. These curves deviate slightly more from $H(s)$ at high frequencies, but exhibit the same trends as before.

The errors, defined as the difference between the dB values of $H(s)$ and $H(z)$ at each frequency, are plotted in Fig. 10 for $f_s = 20$ kHz and $f_s = 44.1$ kHz (abbreviated as 44k) for the settings of t, m, and l that give the worst case results. The error is only meaningful for frequencies up through $f_s/2$.

The curves for $t = 0.5, m = 0, b = 1$ are characteristic of tone settings that give a high pass response and have error within 0.5 dB for both cases of f_s.

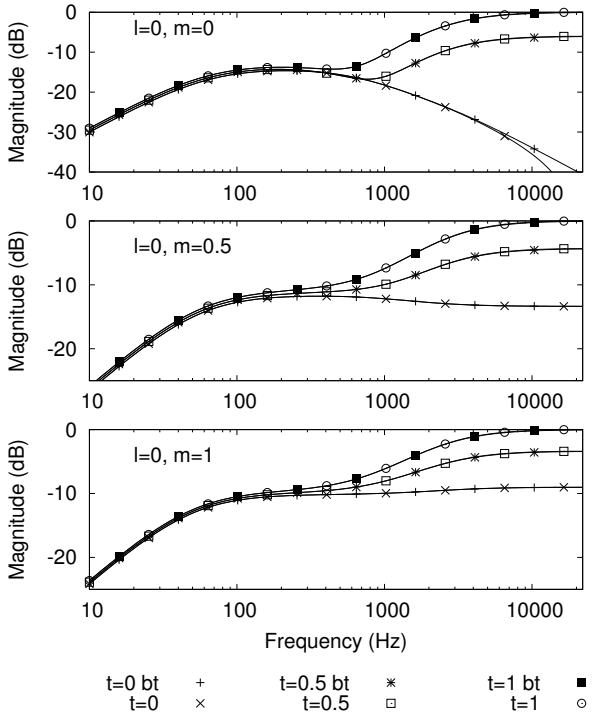

Figure 4: *Comparison of filter magnitude response between original and discretized (*$f_s = 44.1$ *kHz) filters,* $l = 0$.

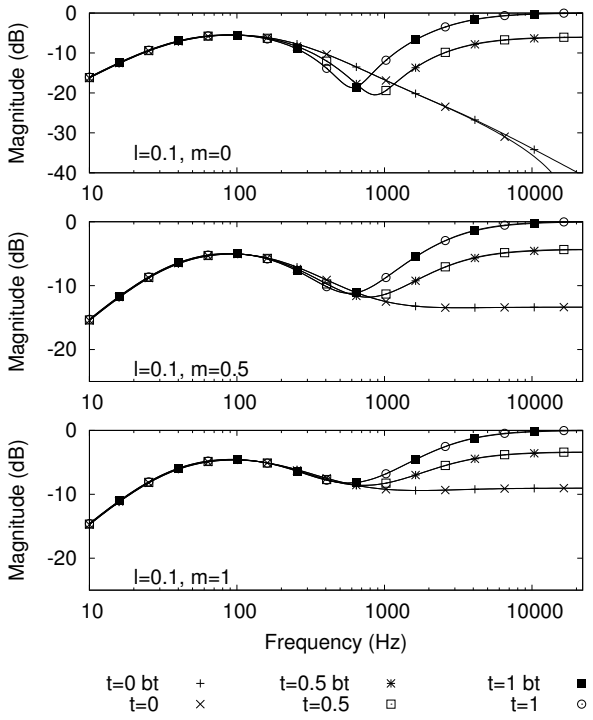

Figure 5: *Comparison of filter magnitude response between original and discretized (*$f_s = 44.1$ *kHz) filters,* $l = 0.1$.

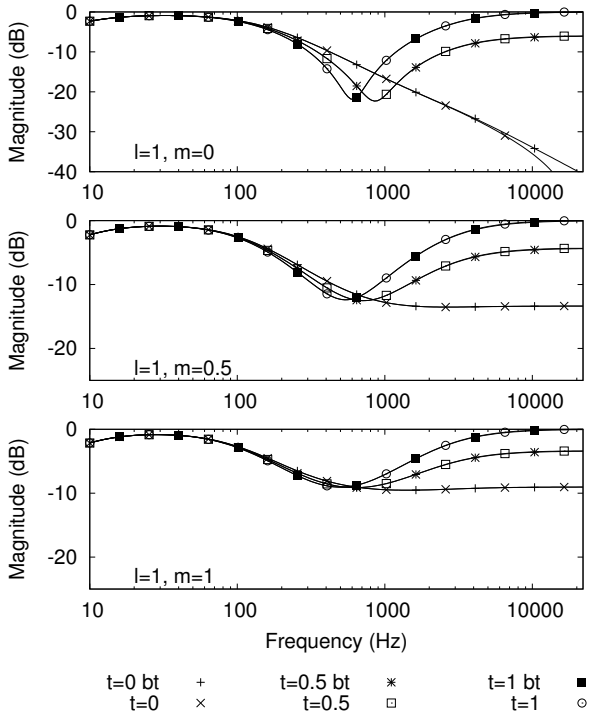

Figure 6: *Comparison of filter magnitude response between original and discretized ($f_s = 44.1$ kHz) filters, $l = 1$.*

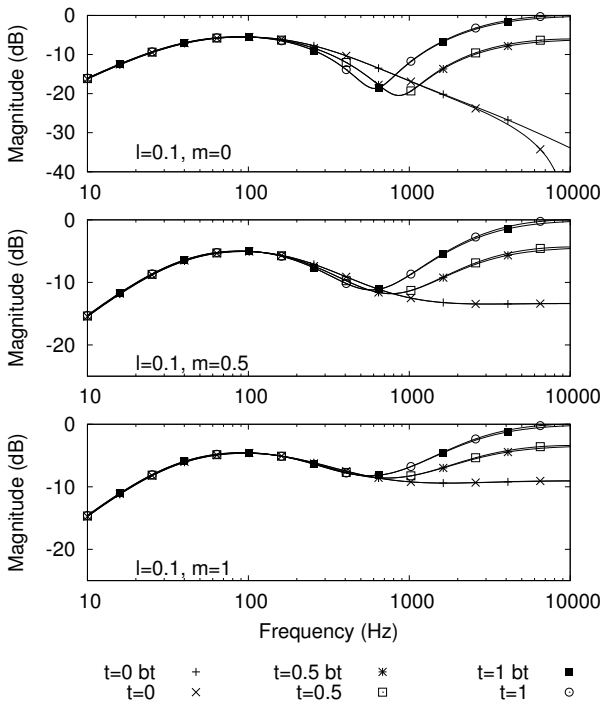

Figure 8: *Comparison of filter magnitude response between original and discretized ($f_s = 20$ kHz) filters, $l = 0.1$.*

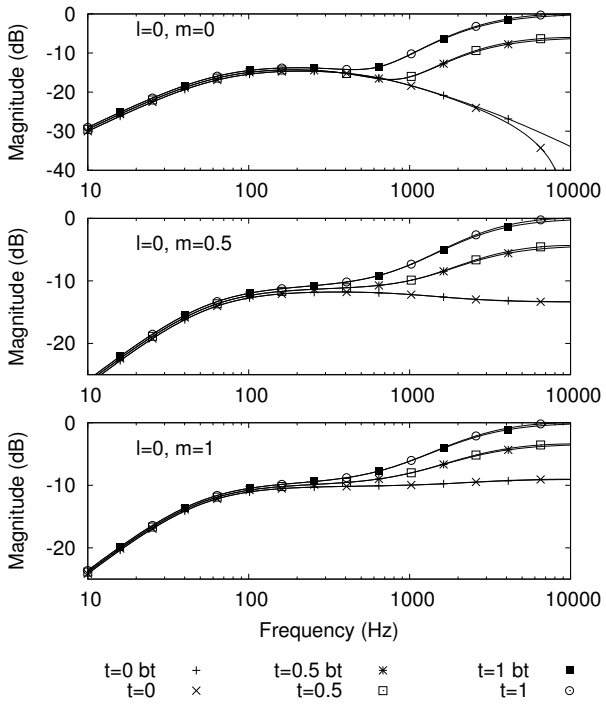

Figure 7: *Comparison of filter magnitude response between original and discretized ($f_s = 20$ kHz) filters, $l = 0$.*

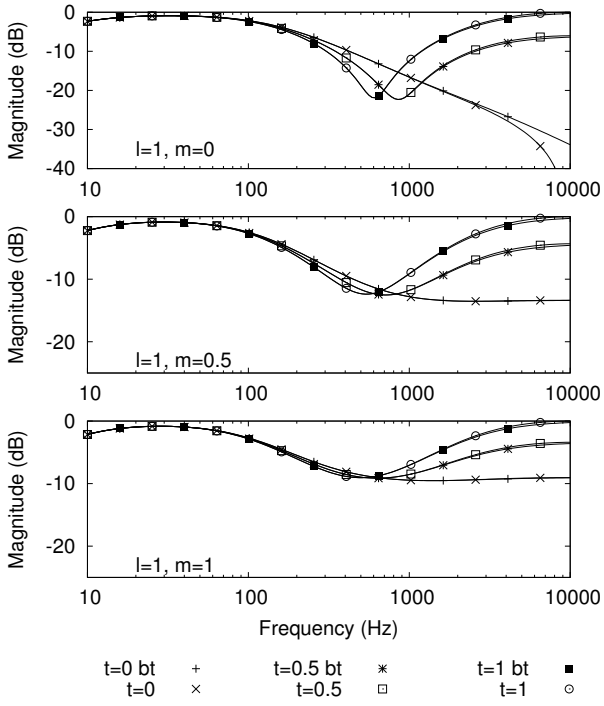

Figure 9: *Comparison of filter magnitude response between original and discretized ($f_s = 20$ kHz) filters, $l = 1$.*

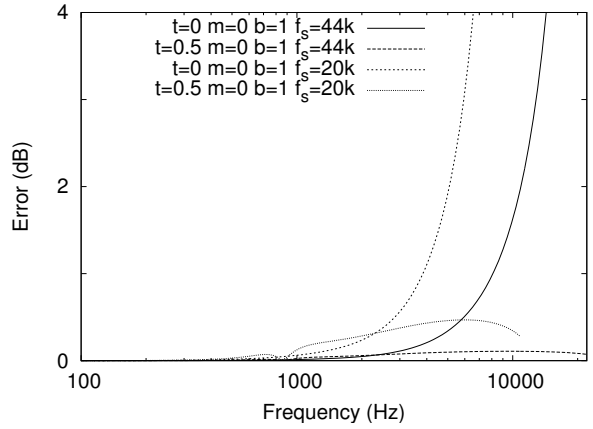

Figure 10: *Error as difference between dB values of $H(s)$ and $H(z)$, for $f_s = 20$ and 44.1 kHz, and the noted tone settings.*

The curves for $t = 0, m = 0, b = 1$ are characteristic of settings that give a low pass response and exhibit a rapidly increasing error as frequency increases because the bilinear transform maps the null at infinite frequency to $f_s/2$. The error rises to 3 dB at roughly 6 kHz for $f_s = 20$ kHz, and at 13 kHz for $f_s = 44.1$ kHz. Because of the low pass nature of these responses, the errors occur at frequencies where the magnitude is at least 10-20 dB lower than its peak value, making them perceptually less salient. Also, given that the frequency response of a typical guitar speaker is from 100 Hz to 6000 Hz, the deviations at higher frequencies would be inconsequential.

3.2. Implications of system poles and zeros for filter implementation

The plots exhibit the complex dependence of the frequency response upon the tone controls. The most obvious effect is that changes in the *Middle* control also affect the treble response. The analytical form of the transfer function provides a way to find the poles and zeros of the system as the settings are varied and gives insight into how the filter could be simplified to facilitate the implementation while maintaining accuracy.

Note that the tone stack is an entirely passive circuit composed of resistors and capacitors. This implies that the three poles of this system are all real. There is a zero at DC, leaving a pair of zeros that may be complex depending on the control settings. This also implies that the tone stack cannot be a resonant circuit although the pair of imaginary zeros can set up an anti-resonance as evident in the notch seen in the frequency response plots.

Also note from Eqn. (1) that none of the coefficients of the denominator depends on the treble control, t. The treble control therefore does not control the modes of the circuit but only adjusts the position of the zeros. This circuit can be decomposed into a weighted sum of terms that correspond to each mode by the partial fraction expansion. From this perspective, the treble control only affects the weighting of the different modes, but not the pole location of each mode. The poles are controlled exclusively by the bass and middle knobs.

This insight suggests possible alternate filter topologies. Instead of implementing the filter directly as a single third-order filter, one could equivalently use series and parallel combinations of lower order filters. Understanding the poles and zeros of the system, one could make simplifying assumptions, ignoring terms that have little impact on the locations of the poles and zeros.

One implementation would be to find the partial fraction expansion of the transfer function using the expression given and precompute the poles, residues, and direct terms based upon the three-dimensional input space of the tone controls. These terms can be interpolated in the input space and used in the parallel filter structure that arises from the partial fraction expansion.

The existence of an analytical expression for the poles and zeros also informs the choice of c in the bilinear transform. The analytical expression allows the computation of frequency domain features such as local maxima or anti-resonance notches to be matched in the discrete-time domain.

4. CONCLUSIONS

This work shows that the Fender tone stack can be parameterized exactly in the discrete-time domain and that the bilinear transform provides an outstanding frequency mapping for reasonable sampling rates. The transfer function for the physical tone stack was found as a function of its control parameters and component values using symbolic math software. This analysis provides a formula for updating the digital tone stack coefficients in a way that exactly emulates the physical circuit. The symbolic form of the transfer function also allows easy determination of the poles and zeros of the system and guides the design of a filter with simplified coefficients.

Further work remains to factor the expression for the tone stack frequency response and find a structure with simpler expressions for updating the filter. One possible implementation is the wave digital filter. A real-time implementation of the tone stack is also in progress.

5. ACKNOWLEDGEMENTS

David Yeh is supported by the NDSEG fellowship. Thanks to Tim Stilson for help with root loci.

6. REFERENCES

[1] Ampwares, "5F6-A schematic," Retrieved June 29th, 2006, [Online] http://www.ampwares.com/ffg/bassman_narrow.html.

[2] D. V. Curtis, K. L. Chapman, C. C. Adams, and Fender Musical Instruments, "Simulated tone stack for electric guitar," United States Patent 6222110, 2001.

[3] T. Goetze, "caps, the C Audio Plugin Suite," Retrieved June 29th, 2006, [Online] http://quitte.de/dsp/caps.html.

[4] Duncan Amps, "Tone stack calculator," Retrieved June 29th, 2006, [Online] http://www.duncanamps.com/tsc/.

[5] R. Kuehnel, *Circuit Analysis of a Legendary Tube Amplifier: The Fender Bassman 5F6-A*, 2nd ed. Seattle: Pentode Press, 2005. [Online]. Available: http://www.pentodepress.com/contents.html

[6] A. Fettweis, "Wave digital filters: Theory and practice," *Proc. IEEE*, vol. 74, pp. 270–327, Feb. 1986.